NeuroImage: Clinical 25 (2020) 102144

Contents lists available at ScienceDirect

NeuroImage: Clinical

journal homepage: www.elsevier.com/locate/ynicl

Cortical reorganization of lower-limb motor representations in an elite archery athlete with congenital amputation of both arms

Kento Nakagawa[a,b,c], Mitsuaki Takemi[d,e], Tomoya Nakanishi[a,b], Atsushi Sasaki[a,b], Kimitaka Nakazawa[a,*]

[a] Graduate School of Arts and Sciences, The University of Tokyo, 3-8-1 Komaba, Meguro-ku, Tokyo, 153-8902, Japan
[b] The Japan Society for the Promotion of Science, 5-3-1 Kojimachi, Chiyoda-ku, Tokyo, 102-0083, Japan
[c] Faculty of Sport Sciences, Waseda University, 2-579-15 Mikajima, Tokorozawa, Saitama, 359-1192, Japan
[d] Division of Physical and Health Education, Graduate School of Education, The University of Tokyo, 7-3-1 Hongo, Bunkyo-ku, Tokyo, 113-0033, Japan
[e] Japan Science and Technology Agency, PRESTO, 4-1-8 Honmachi, Kawaguchi, Saitama, 332-0012, Japan

ARTICLE INFO

Keywords:
Primary motor cortex
Amputee
Plasticity
Neurorehabilitation
Motor mapping
Paralympic

ABSTRACT

Despite their disabilities, top Paralympic athletes have better motor skills than able-bodied athletes. However, the neural underpinnings of these better motor skills remain unclear. We investigated the reorganization of the primary motor cortex (M1) in a Paralympic athlete with congenital amputation of both arms who holds the world record for the farthest accurate shot in archery (Amputee Archer: AA). We recorded brain activity during contraction of right toe, ankle, knee, and hip joint muscles in the AA and 12 able-bodied control subjects using functional magnetic resonance imaging. The results revealed that M1 activation was more widespread in the AA compared with control subjects during all tasks, and shifted towards the lateral part of the M1 during contraction of toe and knee muscles. We also conducted a motor mapping experiment using navigated transcranial magnetic stimulation. The M1 area receiving stimulation elicited motor-evoked potentials from the toe, lower-leg, and thigh muscles, which were larger in the AA compared with 12 control subjects. Furthermore, the AA's motor maps were shifted towards the lateral side of M1. These results suggest an expansion of lower-limb M1 representation towards the lateral side of M1, including the trunk and upper-limb representations, and an expansion of the area of corticomotor neurons innervating the lower limb muscles in the AA. This unique M1 reorganization could underpin the AA's excellent archery performance in the absence of upper limbs. The current results suggest that Paralympic athletes may exhibit extreme M1 plasticity, which could arise through a combination of rigorous long-term motor training and compensatory M1 reorganization for missing body parts.

1. Introduction

Performances of Paralympic athletes always surprise us, and some are superior to those of top able-bodied athletes. The world record holder of the farthest accurate shot in archery is a Paralympic athlete with congenital amputation of both arms, who manipulates a bow and an arrow with his right foot during archery. In the current study, we hypothesized that the athlete's superior motor skills stem from a reorganization of neural circuits in the brain. Elucidating the neural mechanisms of their motor skills could lead to the development of new protocols for neurorehabilitation and efficient motor training. We investigated reorganization of the primary motor cortex (M1) in a world record holder in archery born without both arms.

Body parts have distinct representations in M1, whereby representations of the lower limb, trunk, arm, hand, and face muscles are arranged from the medial to the lateral direction. The area of motor representation varies with the body part and is associated with its dexterity (e.g., the representation of the lower limbs is smaller than that of hand) (Penfield and Boldrey, 1937). M1 representations can be changed with motor training (Karni et al., 1995; Pascual-Leone et al., 1995; Taubert et al., 2016) or disability such as amputation (Raffin et al., 2016; Simões et al., 2012; Stoeckel et al., 2009). Generally, motor training induces an expansion of the corresponding M1 area in the trained limbs or muscles (Karni et al., 1995; Pascual-Leone et al., 1995; Taubert et al., 2016). Limb amputation induces a reduction in the representation of the amputated body part and

* Corresponding author. Laboratory of Sports Sciences, Department of Life Sciences, Graduate School of Arts and Sciences, The University of Tokyo, Meguro-ku, Tokyo, Japan
E-mail address: nakazawa@idaten.c.u-tokyo.ac.jp (K. Nakazawa).

https://doi.org/10.1016/j.nicl.2019.102144
Received 7 June 2019; Received in revised form 13 December 2019; Accepted 21 December 2019
Available online 24 December 2019

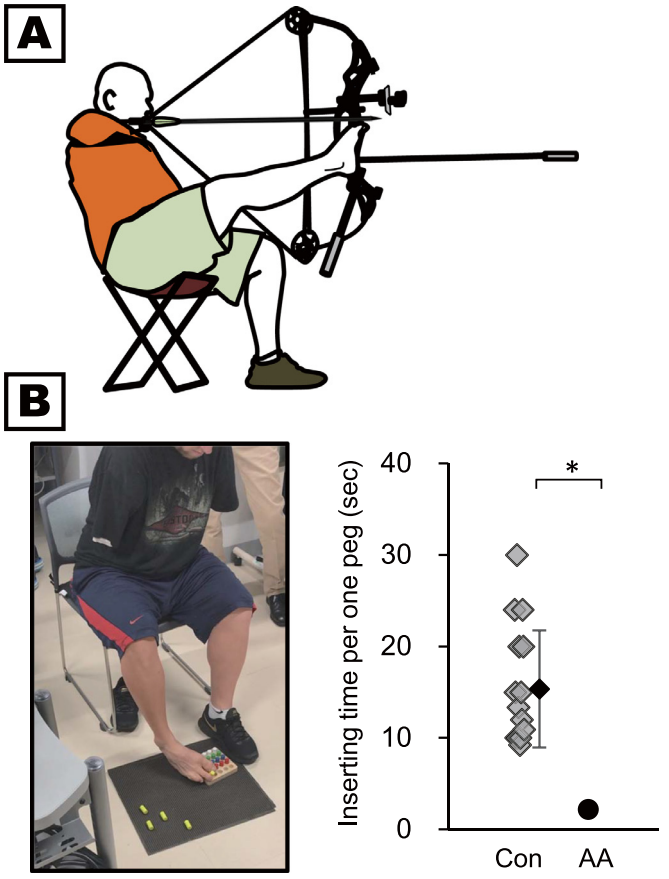

Fig. 1. Amputee archer (AA) and foot dexterity test. (A) The AA manipulates a bow and an arrow with his right foot during archery. *(B)* The peg-board test using the foot (left) in the AA and the corresponding results (right). The gray diamonds and black diamond represent individual data of the control subjects and mean value of the control subjects, respectively. Error bar indicates standard deviation. An asterisk indicates a significant difference between the AA and control subjects (Con).

expansions in the representation of intact body parts towards the amputated body part (Pascual-Leone et al., 1996; Raffin et al., 2016; Simões et al., 2012). This combination of reduction and expansion suggests that the M1 representation of amputated body parts is masked or decayed, and the representation of other intact body parts complements this loss. In addition, brain reorganization depends on the timing of the onset of disability (Kew et al., 1994; Sadato et al., 2002). People with an early onset of disability have been reported to exhibit more dynamic cortical reorganization (Sadato et al., 2002).

The Paralympic athlete we investigated in the current study was a congenital bilateral upper-limb amputee. The athlete uses his lower-limbs to perform archery at world-level competitions, requiring dexterous control of whole lower-limb muscles (Fig. 1A), and also uses the lower-limbs for all daily-life activities. Thus, we hypothesized that the athlete's M1 representation of whole lower limb muscles had expanded towards the lateral part of the M1 (i.e., hand representation). In addition to having congenital amputation, this Paralympic athlete underwent intense motor training, all of which could maximally reinforce cortical plasticity. Thus, this study can tell us about the limits of human brain plasticity.

In the current study, we non-invasively performed mapping of the M1 representations using functional magnetic resonance imaging (fMRI) (Karni et al., 1995; Naito and Hirose, 2014; Raffin et al., 2016; Simões et al., 2012) and transcranial magnetic stimulation (TMS) (Karl et al., 2001; Pascual-Leone et al., 1995, 1996). fMRI can detect task-related changes in the blood-oxygenation-level-dependent (BOLD) signal, and TMS can evaluate the excitability of the existing corticospinal pathway during rest. Thus, fMRI can be used to evaluate functional aspects of neural reorganization, while TMS can be used to evaluate anatomical aspects. Using both methods together can provide complementary information about M1 reorganization.

2. Methods

2.1. Subjects

A 35-year-old archer born without both arms (Amputated Archer: AA) participated in this study. The AA engages in competitive archery using his feet (Fig. 1A), and also uses his feet for daily life activities, such as using a knife and fork and driving a car. The AA started archery training when he was 16 years old, and later participated in the Paralympic games twice. Furthermore, he broke the world record for the farthest accurate shot in archery with a distance of 310 yards.

A total of 19 able-bodied subjects were recruited, and participated in an fMRI experiment (n = 12, 11 male and one female, aged 26.7 ± 3.7 years), a TMS experiment (n = 12, 11 male and one female, aged 26.6 ± 3.6 years), and behavioral testing (n = 13, 11 male and two female, aged 27.6 ± 3.7 years). Four subjects participated in all three experiments. Six subjects participated in fMRI and/or TMS but not behavioral testing.

We confirmed that all subjects were right-handed according to the Edinburgh Handedness Inventory (Oldfield, 1971) (score: 0.89 ± 0.17; a value 1 indicates completely right-handed, and a value of −1 indicates completely left-handed). Furthermore, to determine the dominant foot, subjects were asked which foot they would use to: (i) kick a ball, (ii) stamp out a simulated fire, (iii) pick up a marble, and (iv) trace shapes using their foot (Chapman et al., 1987; Schneiders et al., 2010). Since none of the subjects answered that they use their left foot in these four situations, we judged that all subjects, including the AA, were right-footed. Furthermore, none of the able-bodied subjects had any special experience of dexterous foot movements.

Detailed experimental procedures were explained to the subjects before written informed consent was obtained. This study was approved by the Ethics Committee of the Graduate School of Arts and Sciences, The University of Tokyo (475–2).

2.2. Peg-board test

The peg-board test was conducted to measure foot dexterity. A peg-board consisting of 25 pegs and reservoirs (Color Peg 25, Daiwa, Nara, Japan) was located on the floor in front of subjects, who were seated in a chair. Subjects were instructed to pick up pegs from the floor and to insert each peg into a reservoir with their foot as quickly as possible (Fig. 1B). The number of inserted pegs within 60 s was counted and used to calculate the inserting time per peg. We compared the performance between the AA and control subjects using a two-tailed Crawford and Howell t-test (Crawford and Garthwaite, 2012; Crawford and Howell, 1998), which is a special test designed for comparing a single case to a control sample.

2.3. fMRI experiment

During scanning, subjects lay in the supine position inside the scanner with full knee extension, and only their head was immobilized. Subjects performed four motor tasks involving muscle contraction of the right lower limb in the MRI scanner, as follows: 1) toe: cyclic toe flexion-extension, 2) ankle: cyclic plantarflexion-dorsiflexion, 3) knee: isometric rhythmic contraction of knee extensor muscles, and 4) hip: isometric rhythmic contraction of hip extensor muscles. In each task, subjects were instructed to contract at an approximately 20% effort level to the maximum voluntary contraction. A visual stimulus representing a 1-Hz blinking yellow circle was presented to subjects to

help them maintain the movement frequency, and the task instruction words (e.g., “Toe”) were presented on a black background. Prior to fMRI measurements, subjects practiced the four tasks outside the MRI room.

During the fMRI scan, subjects completed three sessions. One session consisted of eight trials (four types of movement × two repetitions) and inter-trial intervals. The order of the tasks was counter-balanced across sessions but not participants. The task period and inter-trial interval period each lasted for 20 s. Each session included an 8-s dummy scan and a 20-s rest period before the first trial and after the last trial. Thus, each session took 348 s in total.

All MRI images were acquired using a 3 T Siemens MAGNETOM Prisma scanner with a 64-channel head coil. BOLD contrast functional images were acquired using T2*-weighted echo planar imaging free induction decay sequences with the following parameters: repetition time 2000 ms, echo time 25 ms, field of view 192 mm × 192 mm (96 × 96 pixels per slice), flip angle 90°, slice thickness 3 mm, and gap 0.75 mm. The orientation of the axial slices was parallel to the AC-PC line.

The raw fMRI data were analyzed using Statistical Parametric Mapping 12 (Wellcome Department of Cognitive Neurology, London, UK) implemented in MATLAB (MathWorks, Natick, MA, USA). Realigned images were normalized to the standard space of the Montreal Neurological Institute (MNI) brain. Smoothing was performed using an isotropic three-dimensional Gaussian filter with full-width at half-maximum of 8 mm. High-pass filters (128 s) were also applied, and low frequency noise and global changes in the signals were removed. The voxel size after preprocessing was 2 × 2 × 2 mm.

The first-level analysis was performed for each subject using a general linear model that included four regressors for tasks (i.e., toe, ankle, knee and hip movement tasks). We constructed a statistical parametric map of the t-statistic, whereby (1) toe movement > rest, (2) ankle movement > rest, (3) knee movement > rest, (4) hip movement > rest. To minimize the effects of head motion artifacts, we included the six head motion parameters as regressors. The statistical threshold for whole brain analysis was set at $p < 0.05$ corrected for family-wise error (FWE).

To quantitatively compare the M1 activity between subjects, we set three types of region of interest (ROI). To evaluate the activation size in the whole M1, we extracted significant voxels within the left precentral gyrus (Functional Connectivity Toolbox, Neuroimaging Informatics Tools and Resources Clearinghouse, USA, https://www.nitrc.org/projects/conn). We also calculated the simple mean coordinates of the voxels in the largest cluster as the center of gravity (CoG). Furthermore, we set ROIs in the M1 hand regions (−32, −24, 58) (Lotze et al., 2000) to check the expansion of the foot area towards the lateral side. Using these MNI coordinates, we additionally calculated the percentage of BOLD signal changes during the task relative to the rest period. In addition, we calculated the number of significantly activated voxels within a box of 20 × 20 × 20 mm around the determined MNI coordinates (Krings et al., 2000; Meister et al., 2005). We also evaluated the expansion of the hand area in the primary somatosensory area (S1) by calculating the number of active voxels within a box of 20 × 20 × 20 mm around the determined S1 ROI (−42, −35, 65) (Buckner et al., 2011). We then compared the differences in the number of activated voxels, the percentage of BOLD signal changes, and the MNI coordinates of the CoG between the AA and the control subjects using the Crawford-Howell *t*-test. Statistical significance was set at $p < 0.05$. The p-value was adjusted by Bonferroni correction with four comparisons (i.e., four tasks).

To determine whether task-related head movements affected the fMRI results, we evaluated head movements by calculating the root mean square value of the volume-to-volume difference in six motion parameters. We then compared the values between the AA and control subjects using Crawford and Howell t-tests with six comparisons. Moreover, to check for movement artifacts, we evaluated the percentage of BOLD signal change at the control site where sensitivity for movement artifacts is high, and no neural activation is expected (i.e., the ventricle: −24, −44, 8 (Abrams et al., 2013)) in each movement condition.

2.4. TMS experiment

2.4.1. Preparation

Surface electromyography signals were recorded from the following muscles: the ankle dorsiflexor (the tibialis anterior; TA), the ankle plantarflexor (soleus; Sol), the toe flexor (flexor digitorum brevis; FDB), the toe extensor (extensor digitorum brevis; EDB), and the knee extensor (rectus femoris; RF) on the right side. The electromyography signals were amplified and bandpass filtered between 15 and 3000 Hz (AB-611J, Nihon Kohden, Tokyo, Japan) and digitized at 4000 Hz using an A/D converter (Powerlab, AD Instrument, Sydney, Australia).

Single-pulse monophasic TMS was delivered with a Magstim 200 stimulator (Magstim, Whitland, UK) through a 70-mm figure-eight coil. The coil position, orientation, and tilt relative to the subject's head were monitored throughout the experiment using TMS navigation (Brainsight version 2.2.8, Rogue Research, Montreal, Canada). During the experiment, subjects were seated in a chair and instructed to keep their whole body relaxed.

2.4.2. Determination of the hotspot

At the beginning of the experiment, we identified the cortical stimulation site at which coil position, orientation, and tilt relative to the subject's head yielded the largest motor evoked potential (MEP) amplitudes from the TA muscle (Weiss et al., 2013). We applied the first stimulation over the left precentral gyrus crown approx. 0.5 to 1 cm apart from the interhemispheric fissure with the coil orientation perpendicular to the course of the interhemispheric fissure (mediolateral current in the brain), the coil tilt tangential to the subject's head, and the TMS intensity at 40% of the maximum stimulator output (MSO). At this standard position, TMS intensity was shifted in steps of 1–5% MSO until TMS had evoked MEPs of the right TA muscle with the averaged peak-to-peak amplitude of >0.5 mV with the three consecutive stimuli at a constant intensity.

Thereafter, the coil was moved 1 cm in the anterior, posterior, medial, and lateral direction while keeping the coil orientation and TMS intensity. The coil tilt was adjusted depending on the coil position in order to put the coil tangential to the subject's head. We acquired three MEPs at each site, and if TMS over one of the four tested sites consistently evoked larger MEPs as compared to the standard position, this site was set as the new standard position. Once we found the new standard position, we decreased TMS intensity in steps of 1% MSO until the average of three MEPs from the right TA muscle became smaller than 0.5 mV. This intensity plus 1% MSO was defined as the new search intensity of the hotspot. We continued these procedures until TMS over the standard position evoked larger MEPs than TMS to the four neighbor sites.

After the definition of the standard position, the coil orientation was changed ± 5° relative to the standard orientation, which was initially perpendicular to the course of the interhemispheric fissure. We acquired three MEPs at each orientation, and if TMS with either of the ± 5° showed larger averaged amplitude, this site was set as the new standard orientation. Otherwise, we defined the present standard coil orientation and position as the hotspot. We continued to examine the optimal coil orientation until the hotspot had been defined. Note that all subjects showed the optimal coil orientation ranging within ± 20° relative to the initial standard orientation.

2.4.3. Determination of the motor threshold

In the present study, we defined the resting motor threshold (RMT) as the lowest TMS intensity that elicited more than five MEPs greater than 50 μV in the TA muscle when 10 stimuli were delivered to the

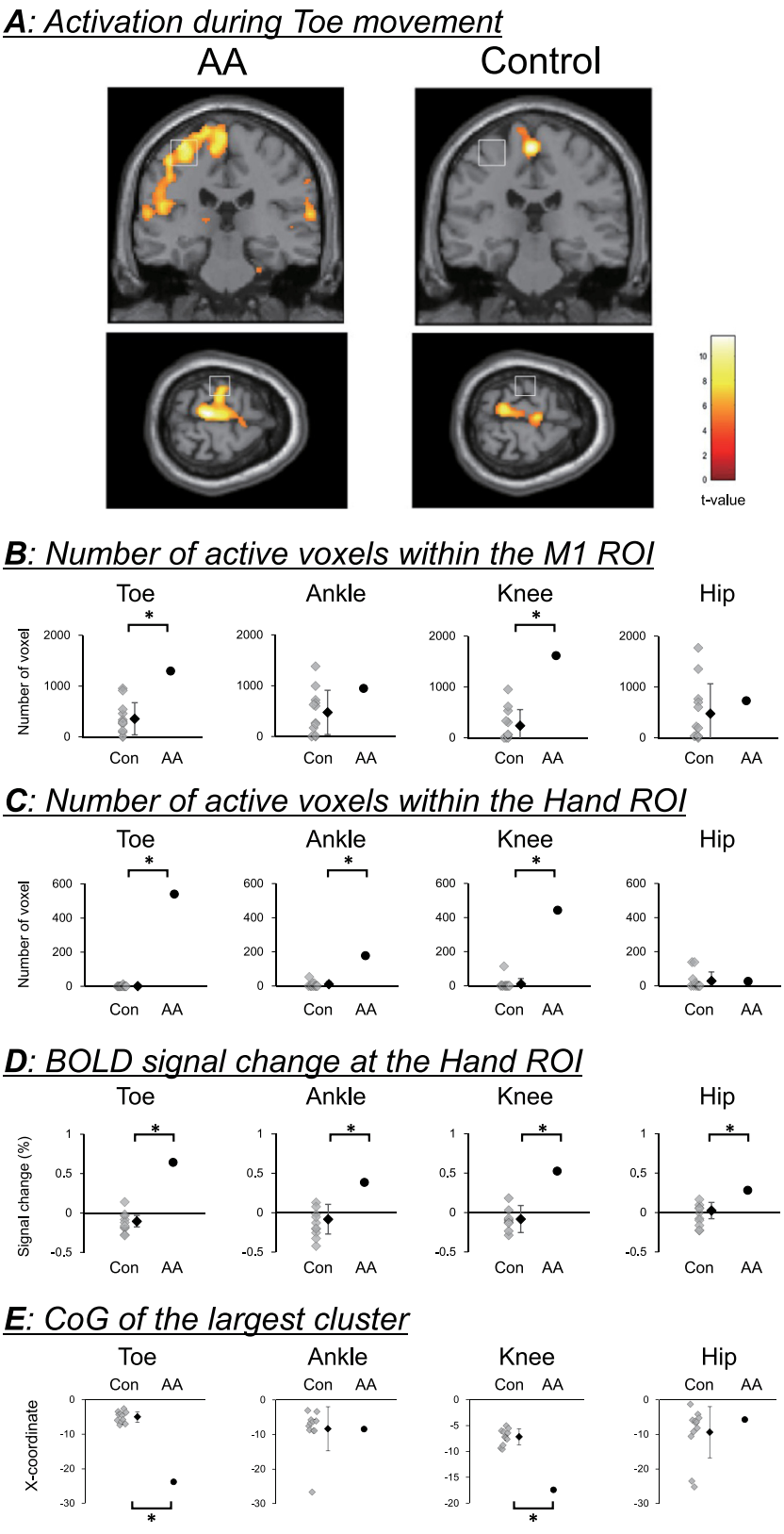

Fig. 2. Mapping of lower-limb representations in fMRI. (A) Brain activity in the AA and one representative control subject during toe movement in the coronal ($y = -26$: upper) and transverse ($z = 72$: lower) sections. The square with a white line represents the boundary of the hand ROI ($-42 < x < -22$, $-34 < y < -14$, $48 < z < 68$ in MNI coordinates). Background images are the MNI template brain images. *(B)* Number of significantly activated voxels ($p < 0.05$ FWE) within the region of interest (ROI) of the M1. *(C)* Number of significantly activated voxels ($p < 0.05$ FWE) within the ROI of M1 hand region. *(D)* Percent signal change of the BOLD response within the ROI of M1 hand region. *(E)* X-coordinate of the center of gravity (CoG) of the largest cluster. The gray diamonds and black diamond represent individual data of the control subjects and the mean value of the control subjects, respectively. Error bars indicate standard deviation. Asterisks indicate a significant difference between the AA and control subjects (Con).

hotspot (Rossini et al., 1994). The first TMS intensity for the RMT determination was set at the last intensity used for the determination of hotspot. We decreased TMS intensity in steps of 1% MSO until less than 5 of 10 stimuli evoked MEP greater than 50 μV. This intensity plus 1% MSO was defined as the RMT (Groppa et al., 2012).

2.4.4. Motor mapping

A motor map was created by delivering TMS with intensity at 120% of the RMT within a rectangular grid defined on the scalp surface. The grid consisted of 10 cm in the mediolateral direction (aligning with the individual optimal coil orientation) and 8 cm in the anteroposterior direction and was (spaced by 1 cm). The center of the grids was

positioned at the hotspot of the TA muscle. Regardless of stimulating points among the grid, the coil orientation was kept stable (according to its orientation at the hotspot). The coil tilt was adjusted depending on the coil position in order to put the coil tangential to the scalp.

Each point of the grid was stimulated with five successive TMS stimuli every 6 ± 0.5 s. The mapping started at the center of the grid and proceeded forward outside of the grid. The next stimulating point was randomly selected from one of the four neighbors of active sites (the average amplitude of five MEPs from the TA was over 50 μV) which had not been stimulated. When the V) which had not been stimulated. When the stimulation induced no response (the average amplitude of five MEPs from the TA muscle was under 50 μV), we deemed the stimulating site as inactive. The mapping was continued until the map was surrounded by inactive sites.

For statistical analysis, the coil positions, orientations, and tilts that were originally determined on the scalp surface were projected to the surface of the brain along the current trajectory. We then aligned the individual T1-weighted image to MNI ICBM 152 average brain using Brainsight software. This allowed us to transform coordinates from the TMS navigation used during the TMS mapping into the common MNI space. As the outputs of Brainsight, we obtained three-dimensional coordinates over the gray-matter surface where the strongest effect of the TMS was expected. The CoG of the motor map in each muscle was calculated for x-coordinate (mediolateral direction) using the following equation:

$$CoG_x = \frac{\sum x_i \times MEP_i}{\sum MEP_i}$$

where MEP_i represents the mean MEP amplitude at one site and x_i represents the MNI normalized coil position in x-coordinates (Fricke et al., 2017). This procedure served to account for individual variations in head size and M1 anatomy (Lotze et al., 2003). The area of motor representation was defined in each muscle using the number of active stimulation sites where the average amplitude of five MEPs was over 50 μV.

Differences in the area of motor representation, CoG, and the coordinates of the hotspot between the AA and control subjects were examined using the Crawford-Howell *t*-test with Bonferroni correction with five comparisons (i.e., five muscles). The criterion for statistical significance was set at $p < 0.05$.

2.5. Follow-up fMRI experiment

To examine the location and size of shoulder representation, we asked the AA and 10 control subjects who participated in the fMRI experiment to conduct a rhythmic abduction-flexion of their right shoulders with a small range at 1 Hz in the MR scanner. We measured BOLD signals during the task. Subjects completed one session consisting of six trials (one task [shoulder movement] × six repetitions) and rest periods. The task and rest period durations each lasted for 20 s. Therefore, the session lasted 260 s. The MR scanner, scanning parameters and preprocessing methods were the same as those used for the main fMRI experiment (the measurement of lower-limb representation). We calculated the number of significantly activated voxels in the largest cluster within the M1 ROI and MNI coordinates of the CoG of the cluster. The results were shown in the supplementary materials.

3. Results

3.1. Peg-board test

The AA inserted all 25 pegs into the halls of the peg-board with his right foot within 60 s, and the average time taken to insert a single peg was 2.2 s (Fig. 1B, Supplementary video). This speed was more than seven times faster than the average speed of control subjects (15.3 s; t [12] = 6.85, $p < 0.001$).

3.2. Lower-limb motor representations in fMRI mapping

Fig. 2A shows the brain activity during the right toe movements for the AA and one representative control subject. Most of the activations in control subjects were located around the medial-wall (foot motor regions). In the AA, although the peak activation of the cluster was located in the M1 region (−6, −36, 72 in MNI coordinates), the cluster around M1 ranged from the medial wall to the temporal lobe. Indeed, the number of significantly activated voxels within the M1 ROI was larger for the AA than control subjects in the toe (t[11] = 21.56, $p < 0.001$) and knee tasks (t[11] = 26.52, $p < 0.001$], but not in the ankle (t[11] = 2.11, $p = 0.23$) and hip tasks (t[11] = 0.89, $p > 0.99$) (Fig. 2B). The number of significantly activated voxels in the M1 hand ROI was also significantly larger for the AA than control subjects in the toe (t[11] = 495.47, $p < 0.001$), ankle (t[11] = 34.39, $p < 0.001$), and knee (t[11] = 41.90, $p < 0.001$) tasks (Fig. 2C), but not in the hip task (t[11] = 0.16, $p > 0.99$). In addition, the task-related changes of BOLD response in the hand ROI were significantly greater for the AA than control subjects in all tasks (toe, t[11] = 20.15, $p < 0.001$; ankle, t[11] = 9.12, $p < 0.001$; knee, t[11] = 15.61, $p < 0.001$; hip, t [11] = 7.34, $p < 0.001$] (Fig. 2D).

Furthermore, we evaluated the spatial shift of lower-limb representation towards the lateral side by comparing x-coordinates of the CoG of the largest activated cluster. The x-coordinate was significantly lower (more lateral) for the AA than control subjects in the toe (t [11] = 36.47, $p < 0.001$) and knee (t[11] = 20.24, $p < 0.001$) tasks (Fig. 2E), but not in the ankle (t[11] = 0.04, $p > 0.99$) and hip (t [11] = 1.57, $p = 0.58$) tasks.

We showed the results of S1 activity, head movements, and the follow up fMRI experiment in the supplementary materials.

3.3. Lower-limb motor representations in TMS mapping

The TMS mapping topographically represents how anatomical pathways from the cortex to spinal motor neurons innervate right lower-limb muscles (Fig. 3A). The size of maps was significantly larger for the AA than control subjects (EDB, t[11] = 8.74, $p < 0.001$; FDB, t [11] = 3.52, $p = 0.022$; TA, t[11] = 8.58, $p < 0.001$; Sol, t [11] = 6.93, $p < 0.001$; RF, t[11] = 4.69, $p = 0.003$] (Fig. 3A and B). The x-coordinate of the CoG was significantly lower (more lateral) for the AA than control subjects for EDB (t[11] = 8.98, $p < 0.001$), TA (t [11] = 20.67, $p < 0.001$), Sol (t[11] = 10.27, $p < 0.001$), and RF muscles (t[11] = 4.04, $p = 0.009$), but not for FDB muscle (t [11] = 2.26, $p = 0.23$) (Fig. 3A and C).

4. Discussion

We investigated M1 reorganization in an elite Paralympic archery athlete born without arms. As expected, the Paralympic athlete's dexterity of lower-limb movement was significantly greater than that of able-bodied control subjects. Our neurophysiological experiments using fMRI revealed a drastic expansion of the athlete's motor representation in a variety of lower-limb muscles. This larger activation in the AA was located not only in the precentral gyrus but also in the postcentral gyrus at the parietal lobe (left bottom in Fig. 2A). However, this effect was also found in control subjects (right bottom in Fig. 2A). Thus, activation in the postcentral gyrus could reflect sensory input from the lower limb, rather than an expansion of motor representation. Furthermore, TMS mapping revealed that the AA had larger M1 regions with corticospinal pathways innervating lower-limb muscles compared with control subjects. In the AA, MEPs were induced from not only the grid points around the foot area, but also those just around or beyond the hand ROI whose x coordinate in MNI coordinates was −32 (e.g., x coordinates of the lateral edge of the map from the EDB: −32, TA: = −40, hand ROI:

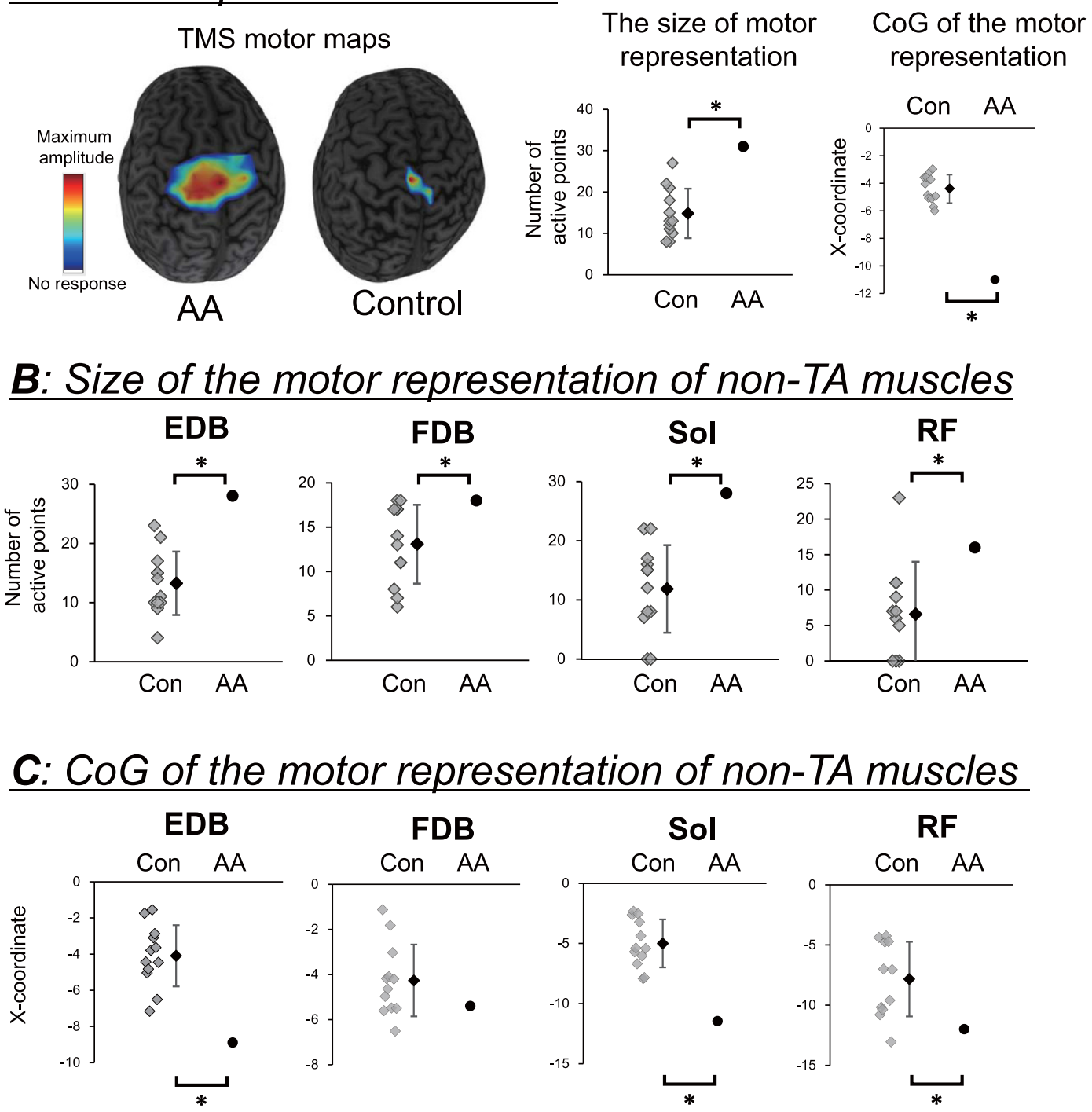

Fig. 3. Mapping of lower-limb motor representation by TMS. (A) Motor representation of tibialis anterior (TA) muscles. TMS motor maps for the AA and the same control subject shown in the left figures. MEP data were normalized to the maximum amplitude in each subject. Each map is superimposed on the un-normalized individual T1-weighted MR image. Spatial interpolation was carried using the natural neighbor interpolation method implemented in the MATLAB "griddata" function. The number of grid points where MEP appeared from TA (the size of motor representation) and the x-coordinates of the center of gravity of the motor presentation of TA were shown in the graphs. The gray diamonds and black diamond represent individual data of the control subjects and the mean value of the control subjects, respectively. Error bars indicate standard deviation. Asterisks indicate a significant difference between the AA and control subjects (Con). *(B)* Size of the motor representation of non-TA muscles. *(C)* X-coordinates of the center of the gravity of the motor representation of non-TA muscles.

−32). The present results suggest that the expanded lower-limb representation towards the lateral side of M1 in the AA subserves his greater archery performance using the lower-limb.

The AA's M1 lower limb representation seems to take over the intact trunk representation as well as the amputated upper limb area. Since the follow-up experiment showed no differences in the size and location of M1 activation during shoulder muscle contraction between the AA and control subjects, the trunk representation in the AA would not appear to be shifted laterally. Therefore, the trunk representation and the expanded lower-limb representation may be overlapped in the AA.

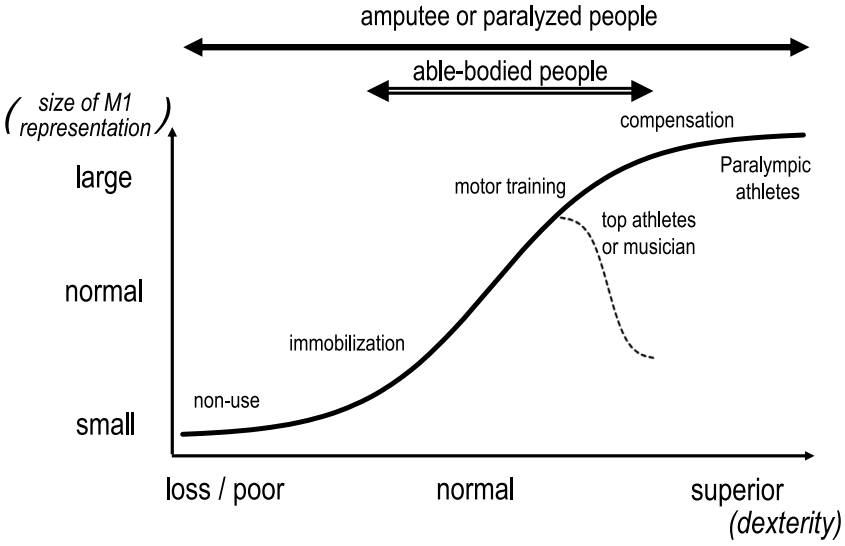

Fig. 4. Schema of M1 reorganization and plasticity. The horizontal axis represents the degree of dexterity of a body part. The vertical axis indicates the direction (expansion and reduction) and size of M1 representation for that body-part. The lined arrow located at the top shows the plausible range of M1 reorganization in disabled people (e.g., limb amputation, spinal cord injury) whose M1 plasticity would be expected to be more drastic than that of able-bodied people, shown by the bottom double-lined arrow. Herein, we propose that Paralympic athletes exhibit the most drastic M1 plasticity by the combination of the expansion in the motor representation for trained body parts and the reduction in adjacent representations through non-use. Top athletes and musicians are thought to show bidirectional changes in motor representations, including expansion and reduction (the branded dotted line), which is commonly referred to as neural efficiency. Note that the sigmoidal curve represents most plausible changes at the population level and does not predict cortical plasticity in each individual.

The AA's ability to stabilize his posture when engaged in archery using the lower-limb might require synergistic recruitment of the trunk and lower limb muscles, leading to a unique M1 reorganization.

Similar to the AA, some control subjects demonstrated weak activation in the secondary somatosensory area (i.e., the right hemisphere of the AA). These activations are likely to have reflected attention to their movement (Kida and Kakigi, 2015), because they were required to perform local muscle contraction without contracting other body parts and to keep the same rhythm to match the guide stimulus.

4.1. Expanded M1 representation and body-part specificity

The fMRI experiment revealed that the AA showed a wide range of M1 activations as well as S1 during toe and knee movements in comparison to control subjects. In addition, the AA showed a larger number of significantly activated voxels in the pre-determined M1 hand area during toe, ankle, and knee movements compared with control subjects. For the ankle task, the number of activated voxels within the whole M1 did not differ between the AA and control subjects while that within the hand ROI was larger in the AA than in control subjects. The difference in the results of the ankle task between M1 ROI and hand ROI might have arisen because the ankle representation in the AA showed lateral expansion without changing the total neural activation volume. Furthermore, task-related changes of the BOLD signal in the hand ROI were larger in the AA than the control subjects in all tasks. A significant difference between the AA and control subjects in the hip task was observed only in the percent signal change, and not in the number of activated voxels. This difference in the hip task results could be because the signal change in the hand ROI in the AA was relatively weaker than in the other tasks and was not sufficient to reach the threshold for the whole-brain analysis. These results suggest that most parts of the lower-limb exhibited expanded motor representations in the AA. Furthermore, the CoG results in the M1 cluster analysis showed that the toe and knee representations, but not the ankle and hip representations, were significantly shifted towards the lateral side compared with controls.

TMS mapping also indicated an expanded M1 lower-limb representation in multiple muscles in the AA. Motor output maps were larger in the AA than controls for all recorded muscles, including the toe, lower leg, and thigh muscles. Furthermore, CoGs of the motor maps in most of the muscles were located on the lateral side in the AA compared with controls. These results suggest that corticomotor neurons connecting spinal motor neurons innervating lower-limb muscles were more widely distributed towards the lateral part of M1 in the AA.

Although the TMS and fMRI experiments both revealed evidence for the expansion of the lower-limb M1 area, the results were not fully consistent. The TMS experiment demonstrated that the innervated regions of all the tested muscles expanded towards the lateral side, whereas the fMRI results showed that significant lateral expansion occurred in the toe and knee motor representations. This discrepancy provides insight into the neural underpinnings of the AA's superior performance, which might be supported by the control of the toe and knee muscles rather than that of the hip and ankle muscles. The findings that S1 expansion was also observed during the toe and knee tasks in the AA also support this possibility. Several previous studies have reported that cortical representations expand when a body part is frequently or dexterously used (Pascual-Leone et al., 1995; Pearce et al., 2000; Philip and Frey, 2014; Taubert et al., 2016). A larger M1 area of upper-limb representation was found to be activated in elite able-bodied archery athletes compared with lower-level archers or novice archers during motor imagery (Callan and Naito, 2014; Kim et al., 2014).

4.2. Schema of M1 reorganization and plasticity

M1 has been found to undergo reorganization after interventions due to the nature of plasticity. Here, we propose a possible scheme of M1 reorganization and plasticity (Fig. 4). Immobilization (e.g., putting a fractured limb in a cast) and non-use (e.g., paralysis, acquired amputation) shrinks the motor representation innervating the affected body part (Freund et al., 2011; Liepert et al., 1995). Cortical representations of intact body parts are expanded following limb amputation, probably due to compensation of missing body parts (Pascual-Leone et al., 1996; Raffin et al., 2016; Simões et al., 2012). In most cases, motor representation expands towards and subsequently will replace the presentation of amputated body parts. Similar compensation-induced M1 expansion in intact body parts has been confirmed in other disorders such as spinal cord injury (Nardone et al., 2013) and stroke (Jones, 2017). We have considered that the compensatory use of an intact body part resulted in its superior dexterity (Nakanishi et al., 2019 in press), much like the Paralympic athlete in the present study.

Furthermore, Yu et al. (2014) suggested that both amputees with and without special skills with an intact body part also exhibit an expansion of M1 representation of the body part, though the size of cortical representation seems larger in those with special skills compared with those without special skills. Thus, motor skills in disabled people appear to be related to the size of M1 representations. Meanwhile, for able-bodied humans, motor training generally induces expansion of the M1 representation of the trained body parts (Karni et al., 1995; Pascual-

Leone et al., 1995). When motor training is continued more extensively in the long-term, the pattern of change in M1 representations appears to be divided into two directions, either expansion or reduction (Callan and Naito, 2014). Some studies have suggested that a shrinking motor representation reflects efficient neural control, as reported in results from an elite soccer player (Naito and Hirose, 2014) and a professional piano player (Krings et al., 2000). In contrast, expanded representations in frequently utilized body parts have been shown for racquetball players (Pearce et al., 2000) and professional musicians (Bangert and Schlaug, 2006). Despite extensive research on cortical reorganization over the last few decades, it remains unclear what factors determine the direction of cortical reorganization associated with the motor experience for able-bodied people.

In the current study, we investigated motor reorganization in a Paralympic athlete. The results indicated unique and drastic M1 representation, possibly greater than that reported in amputated non-athletes in previous studies (Stoeckel et al., 2009). They demonstrated two hotspots for foot muscles in non-athletes with congenital amputation of both arms by using TMS mapping (Stoeckel et al., 2009). In the case of the AA, who was also born without arms, the M1 lower-limb representations appeared to overlap with the intact trunk representation as well as the amputated upper-limb area, resulting in an extremely large lower-limb representation with one hotspot. Taking together, although we cannot directly compare the size of motor representations between the present and previous studies, which evaluated M1 representation with different TMS intensities and lower-limb muscles, Paralympic athletes appear to exhibit the most drastic M1 plasticity with extreme motor skill through a combination of long-term intensive motor training and compensatory M1 reorganization for the missing body parts (Fig. 4).

We propose that since disabled people appear to have a wider range of M1 plasticity than that of able-bodied people, they are able to obtain higher motor skills in the intact body part than able-bodied people. However, the current study evaluated M1 reorganization in a single Paralympic athlete. Thus, we do not yet know whether other elite athletes with sensorimotor disabilities also exhibit extensive M1 reorganization. With our knowledge, we have conducted the only study to reveal M1 plasticity in an elite athlete with a disability, finding that a Paralympic long-jump champion with a below-knee amputation exhibited larger bilateral M1 activation during unilateral knee muscle contraction on the amputated side (Mizuguchi et al., 2019) compared with control participants. This finding supported the notion that unique M1 reorganization occurs in Paralympic athletes and underpins their superb motor skills.

4.3. Limitations

First, neither able-bodied elite archers nor non-athletes with congenital amputation of both arms were included in this study. Comparison of the results in the AA with these two groups in future studies may dissociate the factors of M1 reorganization. Instead, we reviewed previous findings regarding brain reorganization in able-bodied archery athletes (Callan and Naito, 2014; Kim et al., 2014) and amputees of both arms (Stoeckel et al., 2009; Yu et al., 2006, 2014) and proposed a framework of M1 reorganization. However, caution is warranted regarding comparison of the current findings with these previous reports, because the studies used different methodologies. Furthermore, although the present study tested the hypothesis that motor representation in the AA is structured through cortical reorganization and/or plasticity, we cannot exclude the possibility that the AA lacked the M1 hand area congenitally. If so, a different scenario may be involved in the development of the motor representation involving processes other than “plastic change” or “cortical reorganization” through experience.

Regarding the measurement methods, we did not record muscle activities during the fMRI experiment. Thus, we cannot guarantee that the subjects performed the tasks as instructed. Moreover, although we used a traditional TMS mapping method, recent studies have proposed the use of sulcus-aligned TMS mapping, which may be more reliable than the traditional method (Dubbioso et al., 2017; Raffin et al., 2015). Furthermore, we delivered TMS five times at each grid point. This may have been an insufficient number for measuring MEPs, which exhibit trial-to-trial variability, although a previous study reported that a minimum of two TMS stimuli per point is sufficient to obtain valid mapping results (Cavaleri et al., 2017).

Finally, we used whether TMS evoked MEP from the TA muscle as the stop criterion of the TMS mapping. The size of motor representations for the non-TA muscles was not optimally evaluated. One might consider that our findings on the differences in motor representations of EDB, FDB, Sol, and RF muscles between AA and healthy controls are simply due to a small number of tested points. If this were the case, MEP amplitudes of the non-TA muscles should be smaller than the TA when stimulated the same point. Yet, only four of the thirteen subjects showed that averaged MEP amplitudes by the hotspot stimulation were largest for the TA muscle. Thus, significant differences in the motor representations of non-TA muscles between AA and healthy participants should be less affected by intra-individual differences in the number of tested points among lower-limb muscles.

5. Conclusions

An elite archery athlete with congenital amputation of both arms showed (1) an expansion of lower-limb motor representation in M1, especially when performing toe and knee movements, (2) an expansion towards the lateral side of the M1 arching over the trunk and upper-limb representations, and (3) an expanded area of corticomotor neurons innervating the lower-limb muscles. This unique M1 reorganization might underpin the athlete's high level of archery performance using his feet. Furthermore, based on previous findings in non-athletes with both arms amputated (Stoeckel et al., 2009; Yu et al., 2006, 2014) and the present findings, we proposed a framework (Fig. 4) in which the long-term intensive motor training combined with compensatory M1 reorganization for missing/paralyzed body parts leads to the most drastic M1 plasticity, as seen in Paralympic athletes. Based on this framework, the combination of motor training of a body part (e.g., foot) and non-invasive brain stimulation that deactivates the adjacent motor representation (e.g., trunk/hand area) could facilitate the reorganization of non-stimulated M1 regions (e.g., foot area), leading to better neurorehabilitation and motor learning.

CRediT authorship contribution statement

Kento Nakagawa: Conceptualization, Data curation, Formal analysis, Investigation, Validation, Visualization, Writing - original draft, Writing - review & editing. **Mitsuaki Takemi:** Conceptualization, Data curation, Formal analysis, Investigation, Validation, Writing - original draft, Writing - review & editing. **Tomoya Nakanishi:** Data curation, Investigation, Writing - review & editing. **Atsushi Sasaki:** Data curation, Investigation, Writing - review & editing. **Kimitaka Nakazawa:** Conceptualization, Project administration, Supervision, Writing - original draft, Writing - review & editing.

Declaration of Competing Interest

None.

Acknowledgements

We would like to thank Prof. Daichi Nozaki at The University of Tokyo for providing experimental equipment. This work was supported by JSPS KAKENHI Grant Number 18H04082 to K. Nakazawa, the Uehara Memorial Foundation and Japan Broadcasting Cooperation

(NHK). We thank Nia Cason, PhD, and Benjamin Knight, MSc, from Edanz Group (www.edanzediting.com/ac) for editing a draft of this manuscript.

Supplementary materials

Supplementary material associated with this article can be found, in the online version, at doi:10.1016/j.nicl.2019.102144.

References

Abrams, D.A., Lynch, C.J., Cheng, K.M., Phillips, J., Supekar, K., Ryali, S., Uddin, L.Q., Menon, V., 2013. Underconnectivity between voice-selective cortex and reward circuitry in children with autism. Proc. Natl. Acad. Sci. U S A 110, 12060–12065.

Bangert, M., Schlaug, G., 2006. Specialization of the specialized in features of external human brain morphology. Eur. J. Neurosci. 24, 1832–1834.

Buckner, R.L., Krienen, F.M., Castellanos, A., Diaz, J.C., Yeo, B.T., 2011. The organization of the human cerebellum estimated by intrinsic functional connectivity. J. Neurophysiol. 106, 2322–2345.

Callan, D.E., Naito, E., 2014. Neural processes distinguishing elite from expert and novice athletes. Cogn. Behav. Neurol. 27, 183–188.

Chapman, J.P., Chapman, L.J., Allen, J.J., 1987. The measurement of foot preference. Neuropsychologia 25, 579–584.

Crawford, J.R., Garthwaite, P.H., 2012. Single-case research in neuropsychology: a comparison of five forms of *t*-test for comparing a case to controls. Cortex 48, 1009–1016.

Crawford, J.R., Howell, D.C., 1998. Comparing an individual's test score against norms derived from small samples. Clin. Neuropsychol. 12, 482–486.

Dubbioso, R., Raffin, E., Karabanov, A., Thielscher, A., Siebner, H.R., 2017. Centre-surround organization of fast sensorimotor integration in human motor hand area. Neuroimage 158, 37–47.

Freund, P., Weiskopf, N., Ward, N.S., Hutton, C., Gall, A., Ciccarelli, O., Craggs, M., Friston, K., Thompson, A.J., 2011. Disability, atrophy and cortical reorganization following spinal cord injury. Brain 134, 1610–1622.

Fricke, C., Gentner, R., Rumpf, J.J., Weise, D., Saur, D., Classen, J., 2017. Differential spatial representation of precision and power grasps in the human motor system. Neuroimage 158, 58–69.

Groppa, S., Oliviero, A., Eisen, A., Quartarone, A., Cohen, L.G., Mall, V., Kaelin-Lang, A., Mima, T., Rossi, S., Thickbroom, G.W., Rossini, P.M., Ziemann, U., Valls-Sole, J., Siebner, H.R., 2012. A practical guide to diagnostic transcranial magnetic stimulation: report of an ifcn committee. Clin. Neurophysiol. 123, 858–882.

Jones, T.A., 2017. Motor compensation and its effects on neural reorganization after stroke. Nat. Rev. Neurosci. 18, 267–280.

Karl, A., Birbaumer, N., Lutzenberger, W., Cohen, L.G., Flor, H., 2001. Reorganization of motor and somatosensory cortex in upper extremity amputees with phantom limb pain. J. Neurosci. 21, 3609–3618.

Karni, A., Meyer, G., Jezzard, P., Adams, M.M., Turner, R., Ungerleider, L.G., 1995. Functional MRI evidence for adult motor cortex plasticity during motor skill learning. Nature 377, 155–158.

Kew, J.J., Ridding, M.C., Rothwell, J.C., Passingham, R.E., Leigh, P.N., Sooriakumaran, S., Frackowiak, R.S., Brooks, D.J., 1994. Reorganization of cortical blood flow and transcranial magnetic stimulation maps in human subjects after upper limb amputation. J. Neurophysiol. 72, 2517–2524.

Kida, T., Kakigi, R., 2015. Neural mechanisms of attention involved in perception and action: from neuronal activity to network. J. Phys. Fitness Sports Med. 4, 161–169.

Kim, W., Chang, Y., Kim, J., Seo, J., Ryu, K., Lee, E., Woo, M., Janelle, C.M., 2014. An fMRI study of differences in brain activity among elite, expert, and novice archers at the moment of optimal aiming. Cogn. Behav. Neurol. 27, 173–182.

Krings, T., Topper, R., Foltys, H., Erberich, S., Sparing, R., Willmes, K., Thron, A., 2000. Cortical activation patterns during complex motor tasks in piano players and control subjects. A functional magnetic resonance imaging study. Neurosci. Lett. 278, 189–193.

Liepert, J., Tegenthoff, M., Malin, J.P., 1995. Changes of cortical motor area size during immobilization. Electroencephalogr. Clin. Neurophysiol. 97, 382–386.

Lotze, M., Erb, M., Flor, H., Huelsmann, E., Godde, B., Grodd, W., 2000. fMRI evaluation of somatotopic representation in human primary motor cortex. Neuroimage 11, 473–481.

Lotze, M., Kaethner, R.J., Erb, M., Cohen, L.G., Grodd, W., Topka, H., 2003. Comparison of representational maps using functional magnetic resonance imaging and transcranial magnetic stimulation. Clin. Neurophysiol. 114, 306–312.

Meister, I., Krings, T., Foltys, H., Boroojerdi, B., Muller, M., Topper, R., Thron, A., 2005. Effects of long-term practice and task complexity in musicians and nonmusicians performing simple and complex motor tasks: implications for cortical motor organization. Hum Brain Mapp. 25, 345–352.

Mizuguchi, N., Nakagawa, K., Tazawa, Y., Kanosue, K., Nakazawa, K., 2019. Functional plasticity of the ipsilateral primary sensorimotor cortex in an elite long jumper with below-knee amputation. Neuroimage. 23, 101847.

Naito, E., Hirose, S., 2014. Efficient foot motor control by Neymar's brain. Front Hum. Neurosci. 8, 594.

Nakanishi, T., Kobayashi, H., Obata, H., Nakagawa, K., Nakazawa, K., 2019. Remarkable hand grip steadiness in individuals with complete spinal cord injury. Exp. Brain Res. 237, 3175–3183.

Nardone, R., Holler, Y., Brigo, F., Seidl, M., Christova, M., Bergmann, J., Golaszewski, S., Trinka, E., 2013. Functional brain reorganization after spinal cord injury: systematic review of animal and human studies. Brain Res. 1504, 58–73.

Oldfield, R.C., 1971. The assessment and analysis of handedness: the Edinburgh inventory. Neuropsychologia 9, 97–113.

Pascual-Leone, A., Nguyet, D., Cohen, L.G., Brasil-Neto, J.P., Cammarota, A., Hallett, M., 1995. Modulation of muscle responses evoked by transcranial magnetic stimulation during the acquisition of new fine motor skills. J. Neurophysiol. 74, 1037–1045.

Pascual-Leone, A., Peris, M., Tormos, J.M., Pascual, A.P., Catalá, M.D., 1996. Reorganization of human cortical motor output maps following traumatic forearm amputation. Neuroreport 7, 2068–2070.

Pearce, A.J., Thickbroom, G.W., Byrnes, M.L., Mastaglia, F.L., 2000. Functional reorganisation of the corticomotor projection to the hand in skilled racquet players. Exp. Brain Res. 130, 238–243.

Penfield, W., Boldrey, E., 1937. Somatic motor and sensory representation in the cerebral cortex of man as studied by electrical stimulation. Brain 60, 389–443.

Philip, B.A., Frey, S.H., 2014. Compensatory changes accompanying chronic forced use of the nondominant hand by unilateral amputees. J. Neurosci. 34, 3622–3631.

Raffin, E., Pellegrino, G., Di Lazzaro, V., Thielscher, A., Siebner, H.R., 2015. Bringing transcranial mapping into shape: sulcus-aligned mapping captures motor somatotopy in human primary motor hand area. Neuroimage 120, 164–175.

Raffin, E., Richard, N., Giraux, P., Reilly, K.T., 2016. Primary motor cortex changes after amputation correlate with phantom limb pain and the ability to move the phantom limb. Neuroimage 130, 134–144.

Rossini, P.M., Barker, A.T., Berardelli, A., Caramia, M.D., Caruso, G., Cracco, R.Q., Dimitrijevic, M.R., Hallett, M., Katayama, Y., Lucking, C.H., et al., 1994. . non-invasive electrical and magnetic stimulation of the brain, spinal cord and roots: basic principles and procedures for routine clinical application. Report of an IFCN committee. Electroencephalogr. Clin. Neurophysiol. 91, 79–92.

Sadato, N., Okada, T., Honda, M., Yonekura, Y., 2002. Critical period for cross-modal plasticity in blind humans: a functional MRI study. Neuroimage 16, 389–400.

Schneiders, A.G., Sullivan, S.J., O'Malley, K.J., Clarke, S.V., Knappstein, S.A., Taylor, L.J., 2010. A valid and reliable clinical determination of footedness. PM R 2, 835–841.

Simões, E.L., Bramati, I., Rodrigues, E., Franzoi, A., Moll, J., Lent, R., Tovar-Moll, F., 2012. Functional expansion of sensorimotor representation and structural reorganization of callosal connections in lower limb amputees. J. Neurosci. 32, 3211–3220.

Stoeckel, M.C., Seitz, R.J., Buetefisch, C.M., 2009. Congenitally altered motor experience alters somatotopic organization of human primary motor cortex. Proc. Natl. Acad. Sci. 106, 2395–2400.

Taubert, M., Mehnert, J., Pleger, B., Villringer, A., 2016. Rapid and specific gray matter changes in M1 induced by balance training. Neuroimage 133, 399–407.

Weiss, C., Nettekoven, C., Rehme, A.K., Neuschmelting, V., Eisenbeis, A., Goldbrunner, R., Grefkes, C., 2013. Mapping the hand, foot and face representations in the primary motor cortex - retest reliability of neuronavigated TMS versus functional MRI. Neuroimage 66, 531–542.

Yu, X., Zhang, S., Liu, H., Chen, Y., 2006. The activation of the cortical hand area by toe tapping in two bilateral upper-extremities amputees with extraordinary foot movement skill. Magn. Reson. Imaging 24, 45–50.

Yu, X.J., He, H.J., Zhang, Q.W., Zhao, F., Zee, C.S., Zhang, S.Z., Gong, X.Y., 2014. Somatotopic reorganization of hand representation in bilateral arm amputees with or without special foot movement skill. Brain Res. 1546, 9–17.